A Qualitative Visual Servoing
to ensure the Visibility Constraint

Anthony Remazeilles, Nicolas Mansard, François Chaumette
IRISA - INSA and INRIA Rennes
Campus de Beaulieu, 35042 Rennes, France
E-Mail : `Firstname.Lastname@irisa.fr`

Abstract— This paper describes an original control law called *qualitative* servoing. The particularity of this method is that no specific desired value is specified for the visual features involved in the control scheme. Indeed, visual features are only constrained to belong to a confident interval, which gives more flexibility to the system. While this formalism can be used for several types of visual features, it is used in this paper for improving the on-line control of the visibility of a target. The principle is to make a compromise between the classical positioning task and the visibility constraint. Experimental results obtained with a six degrees of freedom robot arm are presented, demonstrating the performance of the proposed method.

I. INTRODUCTION

Visual servoing provides very efficient techniques to control robot motions from an initial position to a precise goal [1], [2]. It supplies high accuracy for the final pose, and good robustness to noise in image processing, camera calibration and other setting parameters. The control loop is based on the minimization of the error between the current and desired values of some visual features. The visibility constraint is one of the critical issues of visual servoing. Indeed, if a large part of the target gets out the camera field of view during the servo, the value of the current features can no more be computed, which leads to a failure of the task. In [3], the loss of some points is accepted and taken into account within the control law, by reducing the contribution of a point while it leaves the camera field of view. This method manages to keep a continuous control law. Nevertheless, nothing avoids the loss of too many points and the task may fail due to the lack of visual information. For example, when considering a visual servoing based on image points, it is well known that at least four points have to be observed [4].

Some control laws have been designed to minimize the risk of visibility loss. When building a partitioned control law, a decoupling is usually done between the centering of the target and the other degrees of freedom (DOF) [5], [6], [7]. With the target at the center of the image, the risk of visibility loss is reduced. Some specific DOF, such as the zoom, can also be added and be devoted to the visibility control [8]. However, the visibility constraint is not taken into account explicitly in the control law but *per se*, by construction of the control scheme. This makes very difficult to take any other constraints into account, such as joint limits, obstacles or visibility loss due to occlusion. In [9], the visibility constraint is explicitly taken into account through a switching control law. At each iteration,

the motion induced by the positioning task is computed. If this motion can lead to a point loss, the controller removes the rotational part of the computed velocity. If a point loss is still expected then the controller requires the robot to translate along the optical axis, getting further to the object and thus increasing the camera field of view. Such a control scheme could be adapted to other kind of constraints (joint limits for example). However, since the robot does not move to minimize the visibility-loss risk but changes its motion when the risk is too high, it is very difficult to adapt this strategy in order to consider several different constraints at the same time.

More generally, the visibility can be treated as a measurable constraint which has to be taken into account when realizing the task. Several strategies have been proposed for controlling the visibility of the features as a minimization problem. A nice solution consists in planning offline the robot trajectory until the desired position while taking into account the visibility constraint, for example using the potential field method [10], [11]. Other constraints can be added and minimized at the same time. However, this combination may induce some local minima. Numerous works have been realized to deal reactively with the minimization of constraints during a positioning task. The major part could easily be adapted to visibility control. See for example [12] for joint-limit and singularity avoidance, or [13] for obstacle and occlusion avoidance. A very suited approach is proposed by the redundancy formalism [14], [15], [16]. The constraints are handled as secondary tasks that are accomplished as long as the main task is not perturbed. It has first been used for visual servoing in [2], and in numerous applications since (e.g. joint limits [17], occlusions [13], etc.). A common lack of these works is the formulation of the secondary task, which is generally *ad hoc* and thus difficult to adapt to other situations. Furthermore, the secondary tasks are realized by the DOF that the main task leaves free. The constraints are thus not taken into account if the main task is full rank (for example in the very common case of positioning the end effector of a 6-DOF manipulator).

When the main task does not let any DOF free, another solution is to realize a trade off between the main task and the constraint [18]. In this case, the control law generates motions that try to achieve the main task and simultaneously take the robot away from its kinematic singularities and its joint limits. Once more, the objective function that represents the constraints is built from *ad-hoc* computations.

In this paper, we propose to control the visibility constraint using a reactive formulation. This constraint is written as a numerical criterion to be minimized by a trade off with the main positioning task. In order to build such a control law, a new formulation called *qualitative servoing* is first proposed. It enables to easily write objectives such as "*the points have to remains away from the image border*" or "*the robot has to stay away from its joint limits*" into a formalism that is commonly used [19]. The control law is defined so that visual features reach a confidence interval. The definition of this new scheme is presented in Section II. Then, it is very easy to integrate it into a classical visual servoing loop. Our solution is very general and can be applied to numerous problems that would have otherwise required tiresome formulations. We propose to apply it to the visibility constraint in Section III. Experimental results, presented in Section IV, demonstrate that this scheme brings significant improvements.

II. QUALITATIVE VISUAL SERVOING

A. Classical visual servoing

A sensor-based robotic task is defined by an error function $\mathbf{e}$, computed from the difference between the current and the desired sensor-based values:

$$\mathbf{e}(\mathbf{p}, t) = \mathbf{x}(\mathbf{p}, t) - \mathbf{x}^*, \tag{1}$$

where $\mathbf{x}$ is the measure vector state computed at the current camera pose $\mathbf{p}$, and $\mathbf{x}^*$ its desired value. If we consider an eye-in-hand robotic system and a static target, the variations of $\mathbf{e}$ are related to the camera motions by:

$$\dot{\mathbf{e}} = \mathbf{L_e}\mathbf{v}, \tag{2}$$

where $\mathbf{v}$ is the instantaneous camera velocity, and $\mathbf{L_e}$ is the interaction matrix describing the variations of $\mathbf{e}$ with respect to $\mathbf{v}$.

A classical control law is obtained by setting an exponential decrease of the error. This is achieved by defining the following differential equation:

$$\dot{\mathbf{e}} = -\lambda\mathbf{e}, \tag{3}$$

where $\lambda \in \mathcal{R}^+$ is used to tune the convergence speed. Combining (2) and (3), a classical control law is obtained [2]:

$$\mathbf{v} = -\lambda\,\widehat{\mathbf{L_e^+}}\mathbf{e}, \tag{4}$$

where $\widehat{\mathbf{L_e^+}}$ is an approximation of the pseudo-inverse of $\mathbf{L_e}$. When the interaction matrix $\mathbf{L_e}$ is full column rank (*ie* rank $\mathbf{L_e} = 6$, all the DOF are controlled), the control law (4) converges locally to an unique position [19].

B. Qualitative visual servoing

Since control law (4) brings the controlled DOF to an unique final position set by $\mathbf{e} = 0$, it is not possible to apply directly such a control law to unfastened constraint such as the visibility constraint. Indeed, the visibility constraint does not correspond to an unique camera pose but is realized in a large region. A first solution to control a robot toward a region

was proposed in [20]. The authors propose a control law that leads the robot end-effector into a region defined by a set of analytical inequalities. Nevertheless, the only feature that can be considered is the end-effector pose, and the extension to visual features is not straightforward. We propose here to develop a control law that manages to bring any kind of vision-based features into a confidence interval.

Contrary to classical visual servoing, the qualitative method requires $\mathbf{e}$ to reach a *confidence interval*, defined by a lower and an upper bound, $\overline{\mathbf{e}}_m$ and $\overline{\mathbf{e}}_M$. The error is thus considered satisfactory if:

$$\forall i \in [1, n], \quad \overline{e}_{m_i} < e_i < \overline{e}_{M_i} \tag{5}$$

In the following, the method presented in Section II-A is used to build a control law that meets this requirement (5), by properly designing a task $\mathbf{e_q}$ from $\mathbf{e}$.

1) With one threshold: In a first time, only the upper bound $\overline{\mathbf{e}} = \overline{\mathbf{e}}_M$ of the confidence interval is considered in order to simplify the equations. The error function $\mathbf{e}_q$ is defined to be:

$$\mathbf{e}_q = \mathbf{H}_{(\mathbf{e}-\overline{\mathbf{e}})}(\mathbf{e} - \overline{\mathbf{e}}), \tag{6}$$

where:

$$\mathbf{H} \quad : \quad \begin{matrix} \mathbf{a}_{1 \times n} & \to & \mathbf{A}_{n \times n} \\ \mathbf{a} & \mapsto & \mathbf{H_a} = diag\left(h_\beta(a_1), \ldots, h_\beta(a_n)\right) \end{matrix} \tag{7}$$

The *activation function* $h_\beta(a)$ defines a continuous transition between 0 and 1. The one used in the following is (see Fig. 1):

$$h_\beta(a) = \begin{cases} 0 & \text{if} & a \leq 0 \\ 1 & \text{if} & a \geq \beta \\ \frac{1}{2}\left(1 + \tanh\left(\frac{1}{1-a/\beta} - \frac{\beta}{a}\right)\right) & \text{otherwise} \end{cases} \tag{8}$$

where β is a positive scalar. This function has been chosen for its nice properties. First it is $\mathcal{C}^\infty$ everywhere (even at the connection points 0 and β). It also remains constant outside the transition interval $]0\,\beta[$ whose length is tuned by parameter β. This means that the space is properly partitioned in three regions: a region where the feature is fully active ($h = 1$), a region where the feature is fully inactive ($h = 0$) and the transient region used to ensure the continuity (this is not the case when using more classical functions such as $arctan$ that are never equal to 0 or 1 but considered so in practice). The parameter β is called *transition smoothness* and is used to tune the trade-off between transition length and effective smoothness (see Fig. 1).

Like in classical visual servoing, the error $\mathbf{e_q}$ can be linked to the camera velocity $\mathbf{v}$ by its interaction matrix $\mathbf{L_{e_q}}$:

$$\dot{\mathbf{e}}_q = \mathbf{L_{e_q}}\mathbf{v} \tag{9}$$

The analytic expression of $\dot{\mathbf{e}}_q$ is easily deduced from (6):

$$\dot{\mathbf{e}}_q = \mathbf{H}_{(\mathbf{e}-\overline{\mathbf{e}})}(\dot{\mathbf{e}} - \dot{\overline{\mathbf{e}}}) + \dot{\mathbf{H}}_{(\mathbf{e}-\overline{\mathbf{e}})}(\mathbf{e} - \overline{\mathbf{e}}) \tag{10}$$

Since $\overline{\mathbf{e}}$ stays constant over time, and if we neglect the transition interval $]0, \beta[$ (that is to say that $\dot{\mathbf{H}}_{(\mathbf{e}-\overline{\mathbf{e}})} \approx \mathbf{0}$), a good approximation of the interaction matrix is obtained:

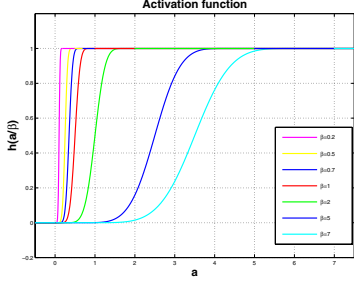$$\mathbf{L_{e_q}} = \mathbf{H}_{(\mathbf{e}-\overline{\mathbf{e}})}\mathbf{L_e} \tag{11}$$

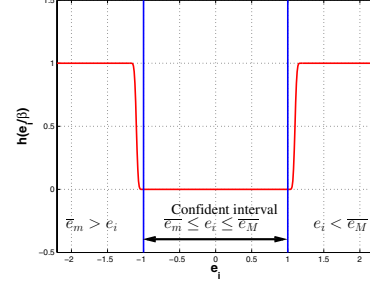Fig. 1. Activation function with different values of the transition smoothness β.

Fig. 2. Control law activation for one component of the measure state $\mathbf{e}$.

Based on (4), the following control law is deduced:

$$\mathbf{v} = -\lambda \left(\mathbf{H}_{(\mathbf{e}-\overline{\mathbf{e}})} \mathbf{L_e} \right)^+ \mathbf{e}_q = \lambda \left(\mathbf{H}_{(\mathbf{e}-\overline{\mathbf{e}})} \mathbf{L_e} \right)^+ \mathbf{H}_{(\mathbf{e}-\overline{\mathbf{e}})} \left(\mathbf{e} - \overline{\mathbf{e}} \right) \quad (12)$$

This control law imposes an exponential decrease of the error $\mathbf{e_q}$. When one feature reaches its confidence interval, the corresponding component of $\mathbf{e_q}$ becomes null. Thanks to the use of the activation matrix into the interaction matrix $\mathbf{HL_e}$, the corresponding line of the interaction matrix is also composed of null terms. The feature is thus not taken into account anymore in the least-square minimization when computing the pseudo-inverse. The control law computed is equal to the control law computed without the inactive feature. The feature can evolve freely into the confidence interval. It is automatically activated again if it leaves the confidence interval due to inner motions.

2) Complete control law: Since the error $\mathbf{e_q}$ is equal to zero beyond the threshold $\overline{\mathbf{e}}$, the previous result can easily be extended to both the lower bound $\overline{\mathbf{e}}_m$ and the upper bound $\overline{\mathbf{e}}_M$ of the confidence interval. The task error $\mathbf{e_q}$ defined in (6) becomes:

$$\mathbf{e}_q = \mathbf{H}_m \left(\mathbf{e} - \overline{\mathbf{e}}_m \right) + \mathbf{H}_M \left(\mathbf{e} - \overline{\mathbf{e}}_M \right), \quad (13)$$

with $\mathbf{H}_m = \mathbf{H}_{(\overline{\mathbf{e}}_m - \mathbf{e})}$ and $\mathbf{H}_M = \mathbf{H}_{(\mathbf{e} - \overline{\mathbf{e}}_M)}$. If all the components of the error bound respect $\overline{e}_m < \overline{e}_M$ (and we of course assume that), then, for each component of $\mathbf{e}_q$, no more than one term of (13) can be activated at a given time: for each component, $h_m \neq 0$ (respectively $h_M \neq 0$)) imposes $h_M = 0$ (resp. $h_m = 0$). This is obvious when considering Fig. 2.

The control law (12) becomes:

$$\mathbf{v} = -\lambda \mathbf{L}_{\mathbf{e_q}}^+ \mathbf{e_q} \quad (14)$$

with:

$$\mathbf{L}_{\mathbf{e}_q} = \left(\mathbf{H}_m + \mathbf{H}_M \right) \mathbf{L_e} \quad (15)$$

If all components belong to their confidence area, then $\mathbf{H}_m = \mathbf{H}_M = \mathbf{0}$, which implies $\mathbf{L}_{\mathbf{e}_q} = \mathbf{0}$. $\mathbf{L}_{\mathbf{e}_q}^+$ is then null, and no camera motion is generated.

As long as visual servoing can manage at the same time different types of visual features, the qualitative features defined in this section can of course be mixed with other classical ones. This will be the subject of Section III.

C. Comparison with other control laws

The introduction of an activation matrix within the control law to activate or inactivate some features is also done in [21], [3]. In these two papers, an activation matrix $\mathbf{H}$ is used to discard non-satisfactory points or outliers. In [21], outliers are points that are badly tracked. By removing these features from the control law, the visual servoing is less sensitive to tracking errors. In [3], the activation matrix enables to reduce continuously the contribution of a point that is getting out the camera field of view, as long as these features can not be tracked and thus updated anymore.

Contrary to these two methods, we propose to reduce then remove the contribution to the control law of a feature that belongs to its confidence interval (that is to say when the error is *close to* zero). This gives more freedom to the features that are still out of their confidence area.

The proposed control law can be applied to different applications. In this paper, it is used for the visibility constraint. Indeed, requiring that a point has to stay within the camera field of view can be expressed as a qualitative feature whose confidence interval corresponds to the image frame. The next section explains how this constraint can be represented using the qualitative servoing method, and how it can be taken into account during a classical image-based positioning task.

III. POINT VISIBILITY CONTROL

In this section, we propose to apply the proposed scheme to the visibility problem by realizing a trade off between a vision-based positioning task and the visibility constraint.

The main task considered here is a positioning task with respect to an object described by a set of points. An image-based visual servoing is used to control the motion of the camera. The basic control law that does not consider the visibility constraint is defined as [2]:

$$\mathbf{v} = -\lambda \widehat{\mathbf{L}}_{\mathbf{x}}^+ \left(\mathbf{x} - \mathbf{x}^* \right), \quad (16)$$

where $\widehat{\mathbf{L}}_{\mathbf{x}}$ is an approximation of the interaction matrix associated to the coordinates of the image points $\mathbf{x_i}$:

$$\mathbf{L_x} = \left(\mathbf{L}_{\mathbf{x}_1}, \dots, \mathbf{L}_{\mathbf{x}_p} \right), \quad (17)$$

and:

$$\mathbf{L_{x_i}} = \begin{bmatrix} -1/Z_i & 0 & u_i/Z_i & u_i v_i & -(1+u_i^2) & v_i \\ 0 & -1/Z_i & v_i/Z_i & 1+v_i^2 & -u_i v_i & -u_i \end{bmatrix},$$
(18)

with $\mathbf{x}_i = (u_i, v_i)$ and Z_i the depth of the corresponding $3D$ point. Different choices are available for $\widehat{\mathbf{L}}$ [22]. We choose $\widehat{\mathbf{L}} = \mathbf{L}^*$ *ie* the interaction matrix computed at the desired position. This choice is frequently done since it provides better camera trajectories and reduces the risk of falling in local minima. Nevertheless, we can not insure that the points will stay inside the camera field of view during all the servo [4]. Next subsection proposes to add some qualitative features to the control law, in order to control and improve the point visibility.

A. Mixing classical and qualitative visual servoing

For each point $\mathbf{x}_i$, a qualitative feature $\mathbf{x_{q_i}}$ is defined. It manages to attract the associated point into a safe area represented in Fig. 3. The positioning task should not be perturbed as long as all the points belong to the safe area. On the opposit, if one point leaves this region, the control law should be adapted in order to get the point back into the safe area.

This notion of safe area corresponds of course to the confident interval of the qualitative servoing. The control law is then obtained by combining the positioning task and the visibility constraints:

$$\mathbf{v} = -\lambda \begin{bmatrix} \mathbf{L_x} \\ \mathbf{L_{e_q}} \end{bmatrix}^+ \begin{bmatrix} \Delta\mathbf{x} \\ \mathbf{e_q} \end{bmatrix},$$
(19)

where $\Delta\mathbf{x} = \mathbf{x} - \mathbf{x}^*$, $\mathbf{L_x}$ is given in (17), while $\mathbf{e_q}$ and $\mathbf{L_{e_q}}$ are defined from respectively (13) and (15):

$$\mathbf{e}_q = \mathbf{H}_m (\mathbf{x} - \overline{\mathbf{x}}_m) + \mathbf{H}_M (\mathbf{x} - \overline{\mathbf{x}}_M),$$
(20)

$$\mathbf{L_{e_q}} = (\mathbf{H}_m + \mathbf{H}_M) \mathbf{L_x}$$
(21)

On one hand, if all points belong to the safe area, then $\mathbf{L_{e_q}} = 0$, since $\mathbf{H}_m = \mathbf{H}_M = \mathbf{0}$. For the same reason, $\mathbf{e_q}$ is null. The control law can then be simplified:

$$\mathbf{v} = -\lambda \begin{bmatrix} \mathbf{L_x} \\ \mathbf{0} \end{bmatrix}^+ \begin{bmatrix} \Delta\mathbf{x} \\ \mathbf{0} \end{bmatrix} = -\lambda \mathbf{L_x^+} \Delta\mathbf{x}$$
(22)

As required, this last equation is the same as the control law without the visibility constraint (16): all the points are in the safe area, and the robot behavior is the one obtained with the classical formalism.

On the other hand, if one point leaves the safe area, the associated qualitative constraint is activated and integrated in the computation of the camera velocity, enforcing a compromise between the positioning task and the visibility constraint.

B. Relaxing the system

Such a control law improves strongly the visibility of the features during the servo (as it will be shown in Section IV). However it is impossible to prove that this visibility is always
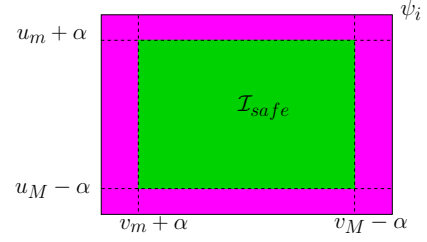

Fig. 3. Safe area $\mathcal{I}_{safe}$ defined within the image ψ_i

ensured. Indeed the positioning task and the visibility constraint are not organized into any hierarchical way. A tradeoff is thus realized between them, which can sometimes result to temporarily feature loss. An example of such a constraint violation is given in the experiment section.

When a point is leaving the confidence area, it seems logical to give more influence to its associated visibility constraint. This can be performed by temporarily removing its contribution to the positioning part of the control law. In this case, we propose to relax the positioning task in an approach similar to [3]:

$$\mathbf{v} = -\lambda \begin{bmatrix} \mathbf{D}\mathbf{L_x} \\ \mathbf{L_{e_q}} \end{bmatrix}^+ \begin{bmatrix} \mathbf{D}\Delta\mathbf{x} \\ \mathbf{e_q} \end{bmatrix},$$
(23)

with $\mathbf{D}$ a diagonal matrix defined as $\mathbf{D} = (\mathbf{I} - \mathbf{H}_m - \mathbf{H}_M)$. If a point $\mathbf{x}_i$ is out of the free area, its associated positioning constraint is reduced to zero ($d_i = 0$).

Once more, if all points belong to the confident area, then $\mathbf{H}_m = \mathbf{H}_M = \mathbf{0}$ and $\mathbf{D} = \mathbf{I}_n$. System (23) is then equivalent to the classical visual servoing system.

IV. EXPERIMENTS

We present in this section two experiments realized with a six-DOF eye-in-hand robot. In each experiment, the robotic system is required to reach a desired pose with respect to a $3D$ object. In order to simplify the image processing, and to focus on the control law validation, the visual target is composed of easily-detectable white dots on black background (see Fig. 4). Experiments involve large camera displacements, and especially large rotations. For such displacements, it is well-known that the camera motions often lead to feature-visibility loss [22].

In the following, two typical experiments are presented. In both experiments, applying a classical control law without visibility control leads some points to leave the camera field of view. Since the $3D$ object model is known, the point position is predicted using $3D$ to $2D$ projections when out of the field of view. The image tracking can thus start again as soon as the point comes back into the image field of view. This scheme enables us to compare the different executions, even if some points get out the image frame.

A. First experiment

For this experiment, the camera displacement is:

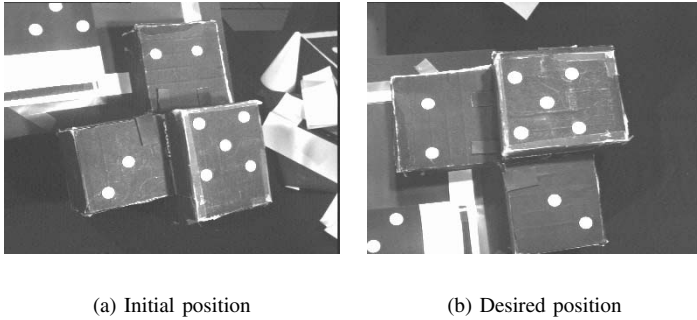$$\mathbf{t} = (-45, -87, 50), \quad \text{and} \quad \mathbf{u}\theta = (-25, -20 -90),$$

(a) Initial position   (b) Desired position

Fig. 4. $3D$ Visual target used in the experiments

where the translation (respectively the rotation) is expressed in cm (resp. dg). Three executions are presented here:

Exp.	β (pixels)	α (pixels)
(a)	No visibility constraint	
(b)	2	25
(c)	15	50

The execution (a) corresponds to a classical visual servoing, using only point features to position the robot. The two others use a qualitative visual servoing to take the visibility constraint into account, as we have proposed in Sec. III-A. Two different tunings of the transition smoothness have been used to illustrate the proper effects of the activation function h defined in (8). In the execution (b), the transition length is very short or abrupt (numerically, it corresponds to an empty interval). Furthermore, the visibility control part is activated when a point is closer than 25 pixel to the image border. The setting (c) provides a smoother transition, and a higher activation threshold.

The experiment is summed up on Figures 5, 6, 7 and 8. The image point trajectories are given in Fig. 5. The classical scheme is not able to keep Points 6 and 7 within the image. The two other schemes which integrate the visibility control (19) manage to keep all the points in the image plane.

The camera trajectories are given in Fig. 6. The two trajectories obtained with (b) and (c) are very similar. The camera enlarges the motion amplitude in order to stay further from the object, which enables to keep all the features in its field of view. One can also see that the trajectory (c) obtained with a long transition length is smoother.

Next figures emphasize the differences between the two parameter sets (b) and (c). The camera velocities are given in Fig. 7. Using a small transition length, the velocities are almost discontinuous at three occasions, when a qualitative feature becomes active or inactive. This leads to very strong accelerations of the robot. These discontinuities do not appear in the case of a proper length setting. The positioning and qualitative errors are presented in Fig. 8. As it was already mentioned on Fig. 5, the positioning errors for settings (b) and (c) are similar. However the qualitative error with abrupt parameters is much lower than for smooth one. As expected, the use of a small transition length leads to abrupt trajectories
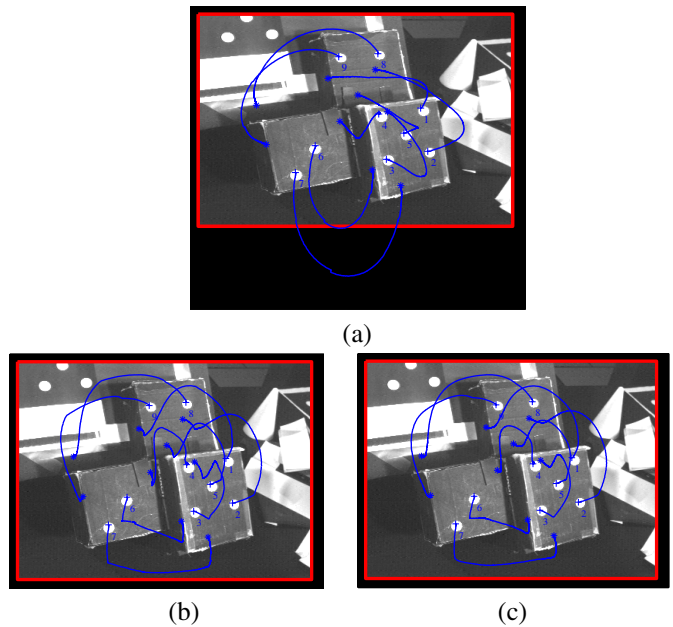

(a)

(b)   (c)

Fig. 5. First experiment. Point trajectories in the image: (a) without considering the visibility constraint (b) with visibility constraints, using an abrupt transition (c) with visibility constraints, using a smooth transition. Two points leave the image frame with the classical visual servoing. The qualitative servoing manages to keep all points within the camera field of view. The image trajectories are quite similar when using smooth or abrupt transition parameters.

and velocities, but makes the system much more reactive. So it is possible to increase the qualitative threshold, enlarging the confident image area in which the visibility constraint is not taken into account.

B. Second experiment - 150 dg Z-rotation

The second experiment mainly consists in a very large rotation around the optical axis. The camera displacement is:

$$\mathbf{t} = (-25, -40, 20), \quad \text{and} \quad \mathbf{u}\theta = (-20, -15, -150),$$

For such a displacement, a classical visual servoing using point features is totally unable to achieve the positioning [22]. Due to a strong coupling in the interaction matrix, the camera translation, which should be very low, involves in fact a very large motion along the optical axis in the direction of the object (see Fig. 10). The loss of two many points causes the failure of the servo (see Fig. 9-(a) for point trajectories). This is a typical case where the visibility is a critical issue.

The results of three experiments are presented here to compare the smoothness of the proposed control law with respect to several setups:

Exp.	β (pixels)	α (pixels)	relaxing
a	No visibility constraint		no relaxing
b	15	50	no relaxing
c	2	25	relaxing
d	15	50	relaxing

Two parameter sets are considered for the qualitative features: a smooth transition (settings (b) and (d)) and an abrupt
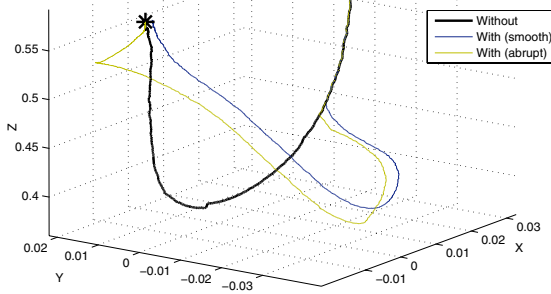
Fig. 6. First experiment. Camera trajectories for the three different schemes. The trajectory obtained using a classical servo looks like a parabola that comes very close to the object. By adding a qualitative part to the control, the camera stays further to the object by increasing the perspective effect. Camera trajectory using a proper transition length is smoother than the one using a short transition length.
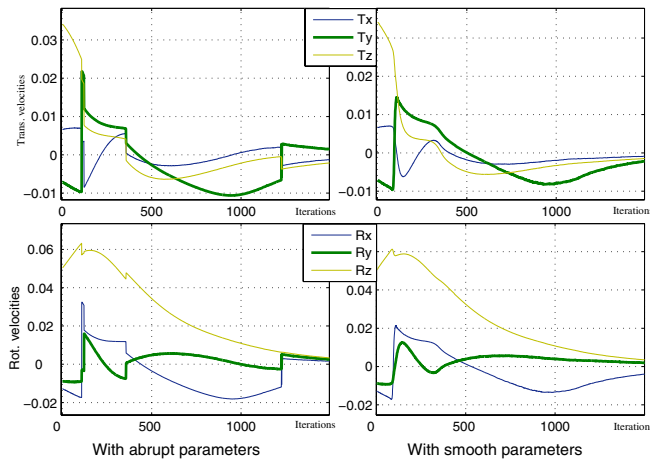

Fig. 7. First experiment. Camera velocities when using a qualitative servo. The velocities are smooth when using a proper transition length, which does not lead to any strong robot acceleration.
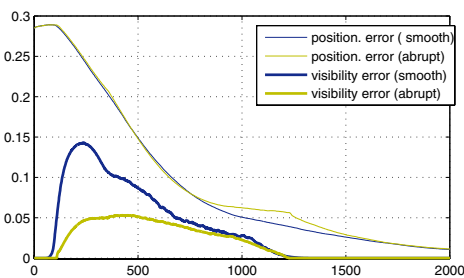

Fig. 8. First experiment. Positioning and visibility error norms. The positioning error is the norm of the vector composed of all point errors. The visibility error is the norm of the vector obtained by stacking all the qualitative feature errors. The more points are close to the image borders, the higher is this error. The positioning errors are similar when using a smooth or an abrupt transition. However, the visibility error is much lower when using a short transient time. The system is then more reactive to correct any visibility problem that may occur.
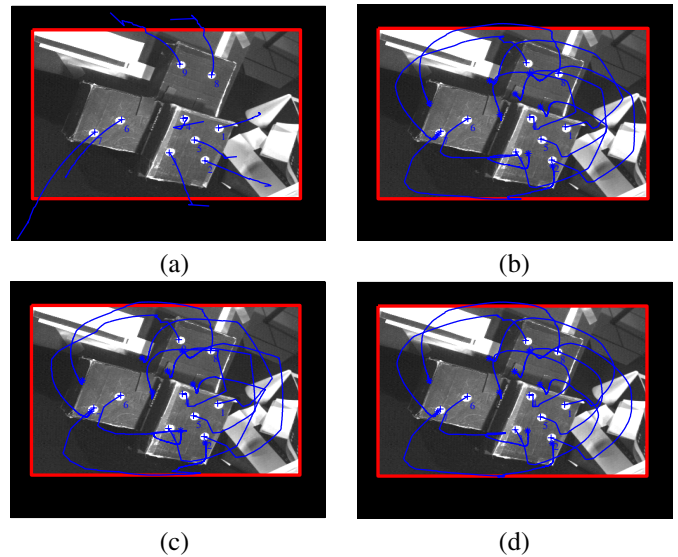

Fig. 9. Second experiment. Point trajectories in the image (a) without taking the visibility constraint into account, (b) with visibility constraints, using a smooth transition and no relax , (c) using an abrupt transition and relax, (d) using a smooth transition and relax. Without any avoidance, the points are quickly lost and the servo fails. Including the visibility constraint, enough points still remain in the image frame to complete the servo. With all the configurations, a point is still lost, and another is border-line. The smoothest trajectories are obtained when using the relaxing strategy (d).

one (setting (c)). The two last settings (c) and (d) use the relaxing strategy as proposed in Sect. III-B.

The executions are summed up on Fig. 9, 10 and 11. Point and camera trajectories are presented on Fig. 9 and 10, including the results from the classical servoing scheme. The positioning task considered is very difficult, and even the controller including the visibility criterion is unable to keep all the points in the field of view. However, the avoidance part of the control law suffices to keep enough point in the image frame to complete the servo. A comparison of the camera velocity smoothness for the three implementations using the visibility constraint is given in Fig. 11. As in the previous experiment, we can see that a short transition implies a more abrupt camera behavior. Furthermore, both points and camera trajectories for the control law without relaxing strategy present some discontinuities (see Fig. 9-(b) and 11). Indeed, the control law is less reactive, and it implies much wider camera motions than when relaxing the lost points (see Fig. 10).

The best execution, in term of smoothness, is obtained with a large transition and with the relax formalism. The combination of a smaller transition and relax gives a very reactive control law, and all point loss can almost be avoided. But this reactivity is obtained at the expense of the motion smoothness.

These experiments show that the relax setup enables in all cases to have a better behavior of the control law. The length of transition leads to a trade-off between smoothness and reactivity, which can be adapted depending on the application considered.
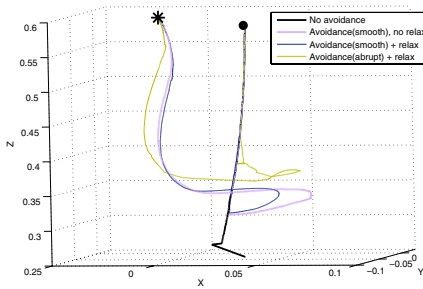
Fig. 10. Second experiment. Camera trajectories in the object frame. Whithout the visibility constraint, large translations along the camera optical axis are performed, due to a strong coupling in the interaction matrix. With the visibility constraint, the camera manages to achieve the task. In this case, the camera trajectory is very abrupt when setting a short transition smoothness and smoother with a higher transition, even without any relax. The camera motion is wider if the relax scheme is not used.
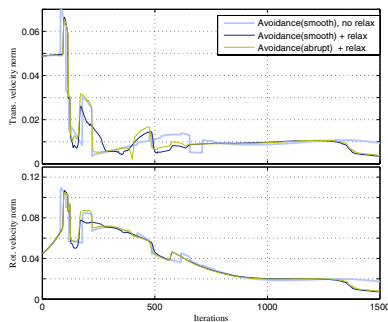

Fig. 11. Second experiment. Camera velocities for the control laws using the visibility constraint. The velocity is very abrupt when using a short transition for the qualitative features or when not using any relax. It is smoother when relaxing the point close to the border and with a long transition.

V. Conclusion

This paper has introduced the principle of qualitative visual servoing. This servo scheme is not defined with respect to a specific desired configuration, but it enables to define a confident interval into which the visual features should remain. A theoretical definition of the qualitative visual servoing has been presented and illustrated with the example of the visibility constraint. The combination of a classical control law with the one proposed enables to realize a compromise between the positioning task and the visibility constraint. It has also been shown that the control law is reduced to the classical one if all the points satisfy the visibility constraint. Experimental results have shown that this formalism manages to greatly improve the feature visibility during the servo. Furthermore, it manages to realize difficult motions that can not be performed by classical vision-based techniques.

The qualitative servoing approach is very general and we are now considering other applications that can benefit from this approach. Indeed, the possibility of adding specific constraints during the servo can be useful for joint-limit avoidance, occlusion avoidance, etc. Furthermore, the possibility of increasing the desired position of a visual feature to an interval is a nice property that could be useful within the redundancy formalism.

The stability analysis of the closed loop should also be studied, doubtlessly by considering the system as a switching control loop.

References

[1] S. Hutchinson, G. Hager, and P. Corke, "A tutorial on visual servo control," IEEE *Trans. on Robotics and Automation*, vol. 12, no. 5, pp. 651–670, Oct. 1996.

[2] B. Espiau, F. Chaumette, and P. Rives, "A new approach to visual servoing in robotics," IEEE *Trans. on Robotics and Automation*, vol. 8, no. 3, pp. 313–326, June 1992.

[3] N. Garcia-Aracil, E. Malis, R. Aracil-Santonja, and C. Perez-Vidal, "Continuous visual servoing despite the changes of visibility in image features," IEEE *Trans. on Robotics*, vol. 21, no. 6, pp. 1214–1220, 2005.

[4] F. Chaumette, "Potential problems of stability and convergence in image-based and position-based visual servoing," in *The Confluence of Vision and Control*, D. Kriegman, G. Hager, and A. Morse, Eds. LNCIS Series, No 237, Springer-Verlag, 1998, pp. 66–78.

[5] P. Corke and S. Hutchinson, "A new partitioned approach to image-based visual servo control," IEEE *Trans. on Robotics and Automation*, vol. 17, no. 4, pp. 507–515, August 2001.

[6] E. Malis, F. Chaumette, and S. Boudet, "2 1/2d visual servoing," IEEE *Trans. on Robotics and Automation*, vol. 15, no. 2, pp. 238–250, Apr. 1999.

[7] V. Kyrki, D. Kragic, and H. Christensen, "New shortest-path approaches to visual servoing," in IEEE *Int. Conf. on Intelligent Robots and Systems*, Sendai, Japan, Oct. 2004, pp. 349–355.

[8] S. Benhimane and E. Malis, "Vision-based control with respect to planar and non-planar objects using a zooming camera," in IEEE *Int. Conf. on Robotics and Automation*, Coimbra, Portugal, July 2003.

[9] G. Chesi, K. Hashimoto, D. Prattichizzo, and A. Vicino, "Keeping features in the field of view in eye-in-hand visual servoing: A switching approach," IEEE *Trans. on Robotics*, vol. 20, no. 5, pp. 908–914, Oct. 2004.

[10] N. J. Cowan and D. E. Koditschek, "Planar image based visual servoing as a navigation problem," in IEEE *Int. Conf. on Robotics and Automation*, Detroit, USA, May 1999, pp. 611–617.

[11] Y. Mezouar and F. Chaumette, "Avoiding self-occlusions and preserving visibility by path planning in the image," *Robotics and Autonomous Systems*, vol. 41, no. 2, pp. 77–87, Nov. 2002.

[12] T.-F. Chang and R.-V. Dubey, "A weighted least-norm solution based scheme for avoiding joints limits for redundant manipulators," IEEE *Trans. on Robotics and Automation*, vol. 11, no. 2, pp. 286–292, Apr. 1995.

[13] E. Marchand and G. Hager, "Dynamic sensor planning in visual servoing," in IEEE *Int. Conf. on Intelligent Robots and Systems*, vol. 3, Leuven, Belgium, May 1998, pp. 1988–1993.

[14] A. Liegeois, "Automatic supervisory control of the configuration and behavior of multibody mechanisms," IEEE *Trans. on Systems, Man and Cybernetics*, vol. 7, no. 12, pp. 868–871, Dec. 1977.

[15] H. Hanafusa, T. Yoshikawa, and Y. Nakamura, "Analysis and control of articulated robot with redundancy," in *IFAC, 8th Triennal World Congress*, vol. 4, 1981, pp. 1927–1932.

[16] B. Siciliano and J.-J. Slotine, "A general framework for managing multiple tasks in highly redundant robotic systems," in *Int. Conf. on Advanced Robotics*, 1991, pp. 1211–1216.

[17] B. Allotta, V. Colla, and G. Bioli, "Kinematic control of robots with joint constraints," *Trans. of the ASME, Journal of Dynamic Systems, Measurement and Control*, vol. 121, pp. 433–442, 1999.

[18] B. Nelson and P. Khosla, "Strategies for increasing the tracking region of an eye-in-hand system by singularity and joint limits avoidance," *Int. Journal of Robotics Research*, vol. 14, no. 3, pp. 163–184, 1992.

[19] C. Samson, M. Le Borgne, and B. Espiau, *Robot control: The Task function approach*. Oxford: Clarendon Press, 1991.

[20] C. Cheah and D. Wang, "Region reaching control of robots: Theory and experiments," in IEEE *Int. Conf. on Robotics and Automation*, Barcelona, Spain, May 2005, pp. 986–992.

[21] E. Marchand, A. Comport, and F. Chaumette, "Improvements in robust 2d visual servoing," in IEEE *Int. Conf. on Robotics and Automation*, vol. 1, New Orleans, USA, Apr. 2004, pp. 745–750.

[22] E. Malis, "Improving vision-based control using efficient second-order minimization techniques," in IEEE *Int. Conf. on Robotics and Automation*, New Orleans, USA, Apr. 2004.